Physica D 437 (2022) 133340

Contents lists available at ScienceDirect

Physica D

journal homepage: www.elsevier.com/locate/physd

On vortex and dark solitons in the cubic–quintic nonlinear Schrödinger equation

Angel Paredes, José R. Salgueiro, Humberto Michinel *

Universidade de Vigo, Applied Physics Department, School of Aeronautic and Space Engineering. As Lagoas s/n, Ourense ES 32004, Spain

ARTICLE INFO

Article history:
Received 25 March 2022
Received in revised form 3 May 2022
Accepted 5 May 2022
Available online 14 May 2022
Communicated by V.M. Pérez-García

Keywords:
Nonlinear Schrödinger equation
Cubic–quintic media
Vortices
Topological charge
Dark solitons
Stability

ABSTRACT

We study topologically charged propagation-invariant eigenstates of the 1+2-dimensional Schrödinger equation with a cubic (focusing)–quintic (defocusing) nonlinear term. First, we revisit the self-trapped vortex soliton solutions. Using a variational ansatz that allows us to describe the solutions as a liquid with a surface tension, we derive a simple formula relating the inner and outer radii of the bright vortex ring. Then, using numerical and variational techniques, we analyse dark soliton solutions for which the wave function density asymptotes to a non-vanishing value. We find an eigenvalue cutoff for the propagation constant that depends on the topological charge l. The variational profile provides simple and very accurate results for $l \geq 2$. We also study the azimuthal stability of the eigenstates by a linear analysis finding that they are stable for all values of the propagation constant, at least for small l.

1. Introduction

Beams carrying angular momentum (i.e.: vortices [1]) are fascinating topological objects [2] present in many branches of physics, from optics [3] or electron beams [4] to coherent matter [5], among many other fields. The nonlinear Schrödinger equation (NLSE) is a paradigmatic model for self-interacting waves and vortices have been widely studied with different versions of it, see e.g. [6,7]. In this framework, vortices are quantized, in the sense that they are defects for which the amplitude of the field vanishes and the phase around the singularity has an integer number of windings l.

The present contribution deals with the NLSE with a focusing cubic and a defocusing quintic nonlinear potential. This model is of substantial theoretical interest because the defocusing term prevents the collapse of the wavefunction that would take place with just the cubic term in dimension two or higher [8], thereby providing an important framework to analyse multidimensional self-trapped fields [9]. Having both focusing and defocusing interactions allows for the existence of both bright and dark stable propagation-invariant soliton-like solutions, a peculiar fact that leads to curious dynamical properties, see e.g. [10]. In particular, there exist stable vortex solitons[1] [15–18]. What happens for solitons with large norm is that they tend to present flat-top profiles, namely the wavefunction has a nearly constant amplitude within a certain region of space whereas it is exponentially vanishing elsewhere. Due to this property, these objects share many qualitative features with liquids [19].

In addition to its appealing mathematical properties, the cubic–quintic model is valuable for the modelling of several physical systems. It has been utilized for quite different situations [20], including plasmas [21], and superfluids [22]. In the context of optical beams, it is useful for laser propagation in certain materials [23] and plays a role in systems with enhanced quintic nonlinearity [24,25] such as an adequately tailored sodium gas [26] (notice that defocusing–focusing cubic–quintic models have also been discussed at length [27]). We must also remark that a cubic–quartic model [28] provides an accurate description of a recently discovered state of matter, the quantum droplets [29,30]. Since the mathematical description of this type of Bose–Einstein condensates shares many similarities with the one discussed in the present paper, the methods presented below might prove useful in that context too.

The purpose of this work is two-fold. First, we revisit the well-studied problem of cubic–quintic vortex solitons by proposing a novel variational ansatz that allows us to write down an effective Hamiltonian for the system as the sum of a bulk term related

* Corresponding author.
E-mail address: hmichinel@uvigo.es (H. Michinel).

[1] Unfortunately, in the literature different and sometimes contradictory denominations are used for the same kind of objects. We use the term vortex soliton [11] for stationary solutions with angular momentum that have a finite support in space. These configurations that have a dark region within a self-trapped bright region are sometimes also called bright spinning solitons [12] or vortex rings [13]. On the other hand, we use the term dark soliton [14] for solutions where the vortex is embedded in an infinite fluid.

https://doi.org/10.1016/j.physd.2022.133340
0167-2789/

to the energy density, a boundary term coming from the surface tension of the "liquid" and a centrifugal term that takes into account the angular momentum. The formalism leads to a simple formula that relates the inner and outer radii of the vortex ring. It turns out that the approximation is qualitative for $l = 1$ but surprisingly precise for $l \geq 2$. Then, we analyse dark solitons with similar methods. We find a one-parameter family of solutions and rigorously prove that a second family of regular solutions with a seemingly allowed asymptotic behaviour does not exist. By adapting to this case the variational procedure, we find again a simple description that is in extremely good agreement with the numerical results for $l \geq 2$ and derive an l-dependent eigenvalue cutoff that, in turn, results in a maximum possible value for the vortex radius. Finally, stability of the stationary states against azimuthal perturbations is studied by a linear analysis complemented by direct numerical simulations.

2. Mathematical model and preliminary remarks

We study the cubic–quintic NLSE model in its dimensionless form:

$$i\frac{\partial \Psi}{\partial z} = -\nabla^2\Psi - (|\Psi|^2 - |\Psi|^4)\Psi \tag{1}$$

where the operator $\nabla^2 = \partial_x^2 + \partial_y^2$ is the Laplacian in two dimensions. All the coefficients can be set to one as in Eq. (1) without loss of generality by appropriately rescaling the wave function and the coordinates x, y, z.

For the NLSE in general there are a number of conserved quantities, including momentum, angular momentum, norm and hamiltonian. We are interested here in the latter two, which we define to be:

$$N = \int |\Psi|^2 dxdy \tag{2}$$

$$H = \int \left(|\vec{\nabla}\Psi|^2 - \frac{1}{2}|\Psi|^4 + \frac{1}{3}|\Psi|^6\right) dxdy \tag{3}$$

Generic propagation invariant eigenstates have the form:

$$\Psi = e^{i\beta z}\psi(x,y) \tag{4}$$

and therefore satisfy the time-independent equation:

$$-\beta\psi = -\nabla^2\psi - (|\psi|^2 - |\psi|^4)\psi \tag{5}$$

In the following sections, we will look for solutions with vorticity of the form:

$$\Psi = e^{i\beta z}e^{il\theta}\psi(r) \tag{6}$$

where r, θ are polar coordinates in the (x, y) plane and $\psi(r)$ is a real function. Using the expression for the Laplacian in polar coordinates, Eq. (5) becomes:

$$-\beta\psi = -\psi'' - \frac{1}{r}\psi' + \frac{l^2}{r^2}\psi - \psi^3 + \psi^5 \tag{7}$$

In Section 3, we will revisit solutions of this equation that are self-trapped vortex rings in which the energy distribution is confined in a region of space $\lim_{r\to\infty}\psi(r) = 0$, which we will call vortex solitons [11]. In Section 4, we consider solutions with $\lim_{r\to\infty}\psi(r) = \psi_\infty \neq 0$, namely dark solitons [14].

Even if this paper is focused in the two-dimensional case, it is useful to recall the explicit one-dimensional (y-independent) kink solution of Eq. (5) [31,32] that will be useful later. The kink solution with propagation constant:

$$\beta = \beta_{cr} = \frac{3}{16} \tag{8}$$

reads:

$$\psi(x) = \frac{\sqrt{3}/2}{\sqrt{e^{\pm\frac{\sqrt{3}}{2}(x-x_0)} + 1}} \tag{9}$$

where x_0 is an integration constant determining the kink position. This solution was first reported, to our knowledge, in ref [33]. For later convenience, let us introduce the width of the kink w_k. We can define it for instance, as the interval in x needed to increase the density $\psi(x)^2$ from 1% to 99% of its maximum, namely $w_k \approx 10.612$.

One-dimensional kink solutions do not exist for other values of β. In order to prove this assertion, let us rewrite the one-dimensional version of (5) as:

$$\frac{d^2\psi}{dx^2} = \beta\psi - \psi^3 + \psi^5 \equiv -\frac{dV}{d\psi} \tag{10}$$

where:

$$V(\psi) = -\frac{1}{2}\beta\psi^2 + \frac{1}{4}\psi^4 - \frac{1}{6}\psi^6 \tag{11}$$

Notice that from (10) is immediate to show that:

$$\frac{d}{dx}\left(\frac{1}{2}\psi'^2 + V\right) = 0 \tag{12}$$

The quantity $\frac{1}{2}\psi'^2 + V$ is therefore constant for all x. We are now interested in kink solutions, such that $\lim_{x\to-\infty}\psi = 0$ and $\lim_{x\to\infty}\psi = \psi_\infty$. From the $x \to -\infty$ limit, we see that $V = 0$. On the other hand, the derivative ψ' must asymptotically vanish as $x \to \infty$, leading to:

$$\beta\psi_\infty - \psi_\infty^3 + \psi_\infty^5 = 0 \tag{13}$$

with two possible solutions:

$$\psi_{\infty,\pm}^2 = \frac{1 \pm \sqrt{1-4\beta}}{2} \tag{14}$$

Moreover, requiring also $V = 0$ at $x \to \infty$, the only non-trivial solution is $\psi_\infty^2 = \psi_{\infty,+}^2 = \frac{3}{4}$, with $\beta = \frac{3}{16}$, namely the one given in (8), (9).

We close this section by commenting on the quantities N, H defined in (3) for the solution (9) (we neglect here the integral over y). Both N and H are of course infinite, but we can regularize them by imposing a cutoff $x_{cut} - x_0 \gg w_k$. We find:

$$N_{cut} = \int_{-\infty}^{x_{cut}} \psi^2 dx = \frac{3}{4}(x_{cut} - x_0) + \mathcal{O}\left(e^{-\frac{\sqrt{3}}{2}(x_{cut}-x_0)}\right)$$

$$H_{cut} = -\frac{9}{64}(x_{cut} - x_0) + \frac{3\sqrt{3}}{32} + \mathcal{O}\left(e^{-\frac{\sqrt{3}}{2}(x_{cut}-x_0)}\right) \tag{15}$$

This contains the sum of a bulk term in which the Hamiltonian density is $-\frac{9}{64}$ and a boundary term that accounts for the contribution to the Hamiltonian of the transition from the $|\psi| \approx 0$ region to the $|\psi| \approx \sqrt{3}/2$ region. Neglecting exponentially suppressed terms, we see that $H_{cut} + \beta_{cr}N_{cut} \approx \frac{3\sqrt{3}}{32}$.

3. Vortex solitons: a new variational approach

In this section, we study bright vortex solitons that are eigenstates with vorticity of the form (6) and with finite extent, $\lim_{r\to\infty}\psi(r) = 0$. These solutions have been discussed in a number of papers. The existence of stable $l = 1$ eigenstates was discovered in [15]. This was generalized for $l = 2$ in [12,16] and for larger values of l in [18,34,35]. In the case of relatively large vorticity, and dominant quintic self-defocusing nonlinearity, the simple Thomas–Fermi (TF) approximation may be quite relevant for the dark vortices [36].

Variational approaches have been successfully developed since long ago for different situations to find approximations to features of many profiles of self-trapped solitons, being probably the most famous the well-known unstable "Townes soliton"[37]. For instance, building on arguments of [38], the authors of [39] could predict the norm of the generalization of the Townes profile to cases with topological charge. One can think about those solutions with self-similar collapse as appearing in a limit of the cubic–quintic model in which the quintic term is vanishingly small. Notice however that the variational approach developed in the present paper is valid in a different regime, since the emergence of the liquid-like phase requires the competition of the cubic and quintic terms.

It turns out that for every $l \geq 1$ there is a value $\beta_{st}(l)$ of the propagation constant such that in the interval $\beta_{st}(l) < \beta < \beta_{cr}$ the vortex solitons are stable. In this region, ψ has a flat-top profile, with the size of the flat region growing as β approaches the eigenvalue cutoff provided by β_{cr}, above which solutions do not exist [40].

Even if vortex solitons in the cubic–quintic model are therefore well understood, we will put forward a novel variational ansatz that will allow us to lay out a new perspective on the problem and to provide a simple yet accurate relation between the inner and outer radii of the rings. Moreover, the type of ansatz introduced below will prove also very useful to describe the dark solitons of Section 4.

It is well known that for the cubic–quintic model (1) there are flat-top eigenstates, namely propagation-invariant states that have almost constant amplitude $|\psi(\mathbf{x})| \approx A$ in a (bulk) region of space of surface S. Away from that region, the solution has almost vanishing amplitude $\psi(\mathbf{x}) \approx 0$. In the boundary of the region, there is a non-trivial profile connecting both regions. In general, for fixed norm and angular momentum, the profile minimizing the Hamiltonian provides a solution. In a first approximation, when the norm N is large and therefore the surface S is large, the value of the Hamiltonian is dominated by the bulk term and the boundary terms would be subleading. Neglecting any such boundary term, we find:

$$H \approx \int \left(-\frac{1}{2}A^4 + \frac{1}{3}A^6\right) d^2\mathbf{x} = S\left(-\frac{1}{2}A^4 + \frac{1}{3}A^6\right) \tag{16}$$

On the other hand, the norm is $N \approx SA^2$ and therefore $H \approx N\left(-\frac{1}{2}A^2 + \frac{1}{3}A^4\right)$. Minimizing this expression for fixed N yields:

$$A_{cr} = \frac{\sqrt{3}}{2}, \qquad \beta_{cr} = \frac{3}{16} \tag{17}$$

where β_{cr} was found directly from Eq. (5) from which $-\beta_{cr} = -(A_{cr}^2 - A_{cr}^4)$. This coincides with the one-dimensional result (8). In fact, this result is valid for any dimension and does not depend on angular momentum and therefore the amplitude and propagation constant for any finite flat-top solution of the cubic–quintic model should tend to (17) when the flat region is asymptotically large. Notice, however, that this argument implicitly assumes that S is finite and therefore does not apply to dark solitons, as the ones that we will analyse in Section 4.

As this reasoning suggests and as it was shown in [18], Eq. (7) admits flat-top solutions for any value of l when β approaches β_{cr}. These solutions look like rings with interior radius R_{int} and exterior radius R_{ext}. For $r \ll R_{int}$ and $r \gg R_{ext}$ we have $\psi \approx 0$ and for $R_{int} \ll r \ll R_{ext}$, we have $\psi \approx A_{cr}$. Our goal here is to find new insights on these flat-top profiles and on the values of the interior and exterior radii of the self-trapped vortex. As a variational ansatz,[2] we can approximate the flat-top profile of these vortices with the expressions of the one-dimensional kink, Eq. (9). Let us define a value $r_{cut} = (R_{int} + R_{ext})/2$ that is well inside the flat region (this is only possible if $R_{ext} - R_{int} \gg w_k$). We take:

$$\psi(r) \approx \begin{cases} 0 & (r < r_{min}) \\ \dfrac{\sqrt{3}/2}{\sqrt{e^{-\frac{\sqrt{3}}{2}(r-R_{int})}+1}}, & (r_{min} \leq r \leq r_{cut}) \\ \dfrac{\sqrt{3}/2}{\sqrt{e^{\frac{\sqrt{3}}{2}(r-R_{ext})}+1}}, & (r > r_{cut}) \end{cases} \tag{18}$$

We have also introduced a value $0 < r_{min} \ll R_{int}$ in order to avoid the divergence around $r = 0$ of the integral of the term in H proportional to l^2. Notice that these expressions solve (7) with $\beta = \beta_{cr}$ if we neglect the second and third terms in the right-hand side. The second term is comparatively small if $|\frac{1}{r}\psi'| \ll |\psi''|$ at the kink position, resulting in $w_k \ll R_{int}$ (if that is satisfied, obviously $w_k \ll R_{ext}$ is also true). The third term would be comparatively small if $l^2 \ll r^2$ for the positions for which the vortex has support, namely $l \ll R_{int}$. Thus, the approximation should work in cases with:

$$R_{int} \gg l,\, w_k \tag{19}$$

The next step is to compute the norm and Hamiltonian of Eq. (3) for the variational profile. Using a procedure analogous to the one leading to (15), we find that the norm is:

$$N \approx \frac{3\pi}{4}(R_{ext}^2 - R_{int}^2) \tag{20}$$

This is simply the area of the ring between R_{int} and R_{ext} multiplied by A_{cr}^2. The Hamiltonian is:

$$H = 2\pi \int_0^\infty r \left(\psi'^2 + \frac{l^2}{r^2}\psi^2 - \frac{1}{2}\psi^4 + \frac{1}{3}\psi^6\right) dr \tag{21}$$

We can split this integral in the bulk contribution for $R_{int} < r < R_{ext}$, considering a constant ψ and two boundary contributions around R_{int} and R_{ext} for which the r in the integral can be considered approximately constant and factored out from the integral. We find:

$$H + \beta N \approx 2\pi \left(\frac{3\sqrt{3}}{32}(R_{int} + R_{ext}) + \frac{3}{4}l^2 \log\left(\frac{R_{ext}}{R_{int}}\right)\right) \tag{22}$$

The first term is a boundary term, analogous to the one found in the one-dimensional case (15). It represents a surface tension [42] for the fluid of constant bulk density, thereby leading to properties that resemble those of liquids [19]. The second term comes from the contribution of the angular momentum, integrated between R_{int} and R_{ext}.

The next step is to minimize this quantity for fixed l, N. In order to do that, we can substitute $R_{ext} = \sqrt{R_{int}^2 + \frac{4N}{3\pi}}$ (Eq. (20)), compute the first derivative with respect to R_{int} and then substitute (20) back. Equating the derivative to 0, we find:

$$R_{int} = \frac{8l^2 R_{ext}}{8l^2 + \sqrt{3}R_{ext}} \tag{23}$$

In Fig. 1, we compare the variational ansatz to the exact profile. Concretely, what we do for each example is the following: For given values of l, β, we determine the profile numerically with a standard relaxation method. From the solution, we extract R_{ext} (for consistency with (18), the values of R_{int} and R_{ext} are determined from the numerical profiles looking for the value of r at which ψ^2 is half of its maximum value). Given R_{ext}, the variational approximation is determined by (18) with R_{int} given in (23). It can be appreciated that the variational ansatz is increasingly

[2] Different variational approaches to the same problem were introduced in [18,35,41].

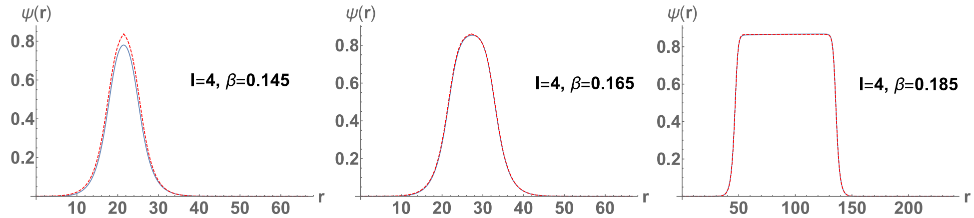

Fig. 1. A comparison of the variational ansatz (18) (red dashed lines) with the numerical approximation to the exact solutions (blue solid lines). We present three examples with $l = 4$ and different values of β.

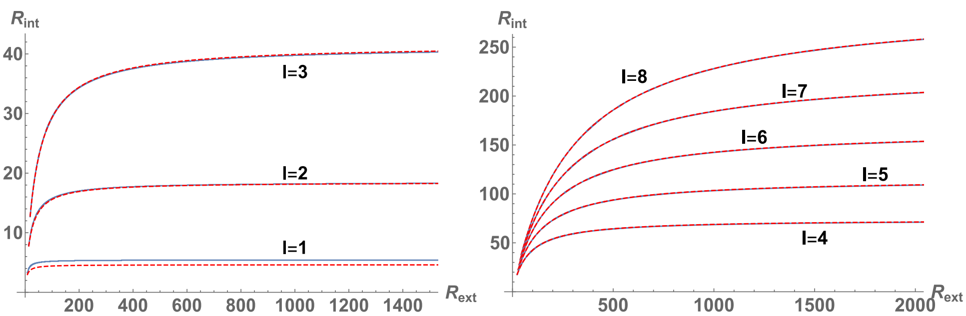

Fig. 2. Internal radius of the ring as a function of the external radius for $l = 1, 2, 3$ (left) and $l =, 4, \ldots, 8$ (right). Solid blue lines are the computed values from the numerical solutions and red dashed lines correspond to the approximate expression (23).

more accurate as β approaches β_{cr} and the profile becomes more clearly flat-top.

In Fig. 2, we compare the prediction (23) with the numerical data as a function of R_{ext} for the lowest values of l. It can be seen that the formula is a very good approximation in all the cases except for $l = 1$, for which it only produces a rough approximation. The inexactitude for the $l = 1$ case can be understood in relation to the failure of the validity condition (19), provided that $R_{int} < w_k$ for any value of R_{ext}. Curiously, the accuracy of the approximate formula (23) for $l \geq 2$, with errors typically well below 1%, is better than what could be expected since it works very well for all the range of β, including values far from β_{cr} for which the profile does not have a flat top and the variational profile (18) does not closely resemble the actual solution.

Let us now briefly comment on the stability of the self-trapped soliton solutions from the point of view of the variational approach. Numerical simulations [18,35] and mathematical arguments [34] have shown that for β near enough β_{cr}, vortices of any value of l are stable. We now present a new perspective on this issue that provides a simple qualitative understanding of the underlying reason.

The result of azimuthal instabilities is typically the disintegration of the vortex eigenstate into several pieces that can be thought of as solitons that fly away from the centre once the vortex has been broken[3] [12,41]. Thus, suppose that there is an instability that ends up breaking the vortex into p pieces, giving rise to a configuration in which the support of the wave function is in several disjoint regions. Now, the optimal case (in the sense of having smaller H) would be that each piece is a soliton, since the soliton is, in fact, the solution of smaller H for a given N. Since the conversion into solitons will never be perfect, the H of the solution will be greater than that of the p solitons that move away from each other. With this in mind, we want to compare the H of the vortex with the H of p solitons. If the H of the solitons is greater than that of the vortex, then the evolution that breaks the vortex will be impossible, which, therefore, should be stable. Requiring that the norm of the vortex soliton is equal to the one of the p resulting solitons yields:

$$N = \pi(R_{ext}^2 - R_{int}^2) = p\pi R_{sol}^2 \tag{24}$$

where R_{sol} is the soliton radius. We can now compare the Hamiltonian of the vortex with the one from the separate solitons by subtracting the surface tension contribution of p solitons to (22), and we get:

$$\begin{aligned}\Delta H &= 2\pi \frac{3\sqrt{3}}{32}\left((R_{int} + R_{ext}) - pR_{sol}\right) = \\ &= 2\pi \frac{3\sqrt{3}}{32}\left((R_{int} + R_{ext}) - \sqrt{p}\sqrt{R_{ext}^2 - R_{int}^2}\right)\end{aligned} \tag{25}$$

We have disregarded terms related to angular momentum since they are subleading. From this equation, it is clear that, when R_{ext} is large enough, ΔH will always become negative (we are requiring $p \geq 2$ taking into account conservation of linear and angular momentum). This shows that a flat-top vortex soliton of any l with large enough N cannot decay into separate solitons. Intuitively, this is very easy to understand: for very large R_{ext}, we have $R_{int} \ll R_{ext}$ and, in fact, the hole in the middle can be almost neglected, the intensity profile of the vortex looks very much like that of a flat-top soliton which, obviously, is not energetically favoured to decay into two or more separate solitons. Notice also that this argument suggests that the last decay mode that remains unstable when R_{ext} grows is $p = 2$, as it was found in [18] by direct numerical integration.

4. Dark solitons

In this section, we deal with solutions of Eq. (7) that asymptotically tend to a non-zero value, $\lim_{r\to\infty} \psi = \psi_\infty$. To the best of our knowledge, these states in the cubic–quintic model have only been briefly discussed in [43]. Clearly, from the $r \to \infty$ limit of the equation, we find the same Eqs. (13) and (14) that we had encountered in the one-dimensional case. It turns out that there are no solutions asymptoting to $\psi_{\infty,-}$ as defined in Eq. (14), as

[3] Another sort of instability for vortex solitons could be the splitting of a higher order topological singularity into several of smaller order. That process is analogous to the one driving instabilities for dark solitons and will be addressed in Section 4, where we show that it does not generate instabilities in the cubic–quintic model at least for large regions of the space of solutions.

we prove in the appendix by making use of Pohozaev's identity. Therefore, we have:

$$\psi_\infty^2 = \psi_{\infty,+}^2 = \frac{1+\sqrt{1-4\beta}}{2} \tag{26}$$

For simplicity of notation, for the rest of this section ψ_∞ stands for $\psi_{\infty,+}$. Unlike for the one-dimensional kink, the value of β is not fixed and there is a continuous family of solutions depending on this parameter. We start by studying this family of solutions with variational methods and comparing the results with the numerical solutions. Then, we present an analysis of the stability properties of these dark solitons in the cubic–quintic NLSE.

4.1. Variational and numerical analysis

Provided the successful variational modelling of vortex solitons in Section 3, it is natural to consider a profile resembling (18):

$$\psi \approx \frac{\psi_\infty}{\sqrt{e^{-a(r-R_{dark})}+1}} \tag{27}$$

We insert this expression into the following Lagrangian,[4] whose Lagrangian density gives rise to Eq. (7), see e.g. [44]:

$$L = 2\pi\int_0^\infty r\left(\psi'^2 + \frac{l^2}{r^2}\psi^2 + \beta\psi^2 - \frac{1}{2}\psi^4 + \frac{1}{3}\psi^6\right) \tag{28}$$

We should fix parameters a and R_{dark} by minimizing L. Since L is divergent, we introduce a cutoff for the integrals r_{cut} that will be later removed. Similarly to Section 3, the Lagrangian can be approximated as the sum of three terms:

$$L \approx L_{surf} + L_{bulk} + L_l \tag{29}$$

where L_{surf} is the surface tension contribution:

$$L_{surf} = 2\pi\frac{\psi_\infty^2}{8a}(a^2 + 4\psi_\infty^2(1-\psi_\infty^2))R_{dark} \tag{30}$$

the term L_{bulk} comes from the integral of the quadratic, quartic and sextic terms:

$$L_{bulk} = 2\pi(\beta\psi_\infty^2 - \frac{1}{2}\psi_\infty^4 + \frac{1}{3}\psi_\infty^6)\frac{1}{2}(r_{cut}^2 - R_{dark}^2) \tag{31}$$

and the L_l term comes from angular momentum:

$$L_l = 2\pi\psi_\infty^2 l^2\log\left(\frac{r_{cut}}{R_{dark}}\right) \tag{32}$$

We can now easily fix a since it only appears in L_{surf}. By cancelling the first derivative, we get

$$a = 2\psi_\infty\sqrt{1-\psi_\infty^2} \tag{33}$$

and therefore $L_{surf} = 2\pi R_{dark}\frac{1}{2}\psi_\infty^3\sqrt{1-\psi_\infty^2}$. Let us now define a renormalized, finite, L_f by subtracting the infinite additive terms including r_{cut}. Notice that those terms do not include R_{dark} and therefore are irrelevant for the determination of that quantity. Putting everything together, we find:

$$L_f = \pi R_{dark}\psi_\infty^3\sqrt{1-\psi_\infty^2} + \pi(-\beta\psi_\infty^2 + \frac{1}{2}\psi_\infty^4 - \frac{1}{3}\psi_\infty^6)R_{dark}^2 \\ - 2\pi\psi_\infty^2 l^2\log(R_{dark}) \tag{34}$$

[4] The procedure of minimizing H for fixed N used in Section 3 is ill-defined here because both quantities are divergent. On the other hand, the computation of Section 3 could have been defined in terms of the Lagrangian, notice that $L = H + \beta N$, cf. Eq. (22).

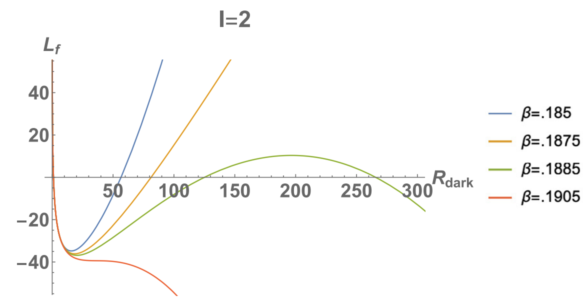

Fig. 3. Examples of the variational Lagrangian with $l = 2$ and different values of β. For $\beta < \frac{3}{16}$, L_f grows quadratically as $R_{dark} \to \infty$ and there is only a local minimum. In the limiting case $\beta = \frac{3}{16}$, L_f grows linearly as $R_{dark} \to \infty$ and there is still only a local minimum. For $\frac{3}{16} < \beta < \beta_{max}(l)$, there exist a local minimum and a local maximum. For $\beta \geq \beta_{max}(l)$ there are no local extrema.

We can rephrase this expression in terms of β by substituting (26). We find:

$$\frac{L_f}{\pi} = \frac{\sqrt{\beta}R_{dark}}{2}(1+\sqrt{1-4\beta}) + \frac{R_{dark}^2}{12}((1-4\beta)^{\frac{3}{2}} + 1 - 6\beta) \\ - l^2(1+\sqrt{1-4\beta})\log(R_{dark}) \tag{35}$$

Notice that $\lim_{R_{dark}\to 0} L_f = +\infty$ because of the centrifugal, logarithmic term. The behaviour at $R_{dark} \to \infty$ depends on the sign of the quadratic term, which is positive for $\beta < \frac{3}{16}$ and negative for $\frac{3}{16} < \beta < \frac{1}{4}$. Thus, for $\beta \leq \frac{3}{16}$ $\lim_{R_{dark}\to\infty} L_f = +\infty$ there is always a global minimum of L_f. For $\frac{3}{16} < \beta < \frac{1}{4}$, we have $\lim_{R_{dark}\to\infty} L_f = -\infty$. It turns out that there is a region of parameter space $\frac{3}{16} < \beta < \beta_{max}(l)$ for which there is a local minimum and a local maximum whereas for $\beta \geq \beta_{max}(l)$ there are no local extrema. Fig. 3 illustrates this point.

By finding the local minimum of L_f, we find:

$$R_{dark} = \frac{-3\sqrt{\beta} + \sqrt{12l^2(1+\sqrt{1-4\beta}-8\beta)+9\beta}}{1+\sqrt{1-4\beta}-8\beta} \tag{36}$$

Thus, for given values of the parameters l and β, the variational approximation is given in Eq. (27) with the values of ψ_∞, a, R_{dark} displayed in Eqs. (26), (33), (36), respectively. In Fig. 4, we show a comparison of these variational profiles with numerical solutions of Eq. (7) found by a standard relaxation method. The graph shows that the approximation is extremely rough for $l = 1$ but works rather well for $l \geq 2$ and gets better for larger values of β.

The radius of the dark hole as given in (36) should be a real positive number in order to have a sensible solution. Therefore, we have to require that the expression inside the square root is positive and this leads to $0 < \beta < \beta_{max}(l)$ with:

$$\beta_{max}(l) = \frac{24l^2(8l^2-1)}{(32l^2-3)^2} \tag{37}$$

Notice also that the value of R_{dark} for $\beta = \beta_{max}(l)$ is finite, leading to a limiting radius:

$$R_{dark} < \frac{l\sqrt{2}(32l^2-3)}{\sqrt{3}\sqrt{8l^2-1}} \tag{38}$$

In figure 5 we show a comparison of Eq. (36) to some values found by numerically computing the eigenstates. Again, we see that the variational approach leads to a rough approximation for $l = 1$ but yields rather accurate predictions for $l \geq 2$ (see Fig. 5).

Reassuringly, it can be checked that the dark soliton with $\beta = \beta_{cr} = \frac{3}{16}$ is the infinite norm limit of the vortex solitons

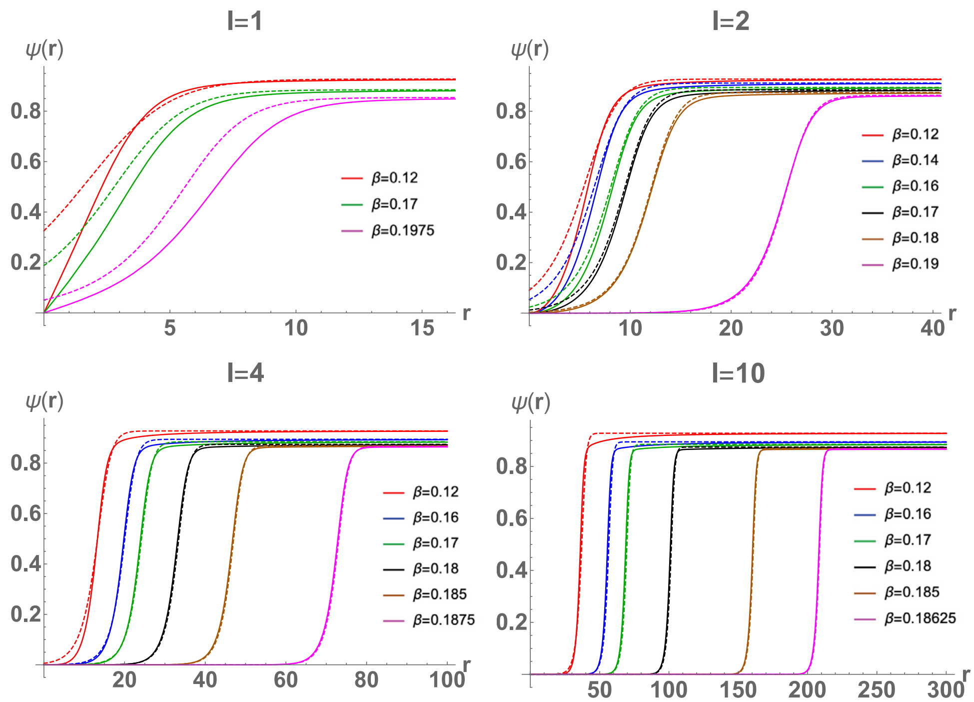

Fig. 4. A comparison of the dark soliton profiles found numerically (solid lines) and the variational approximations (dashed lines) for different values of l and β.

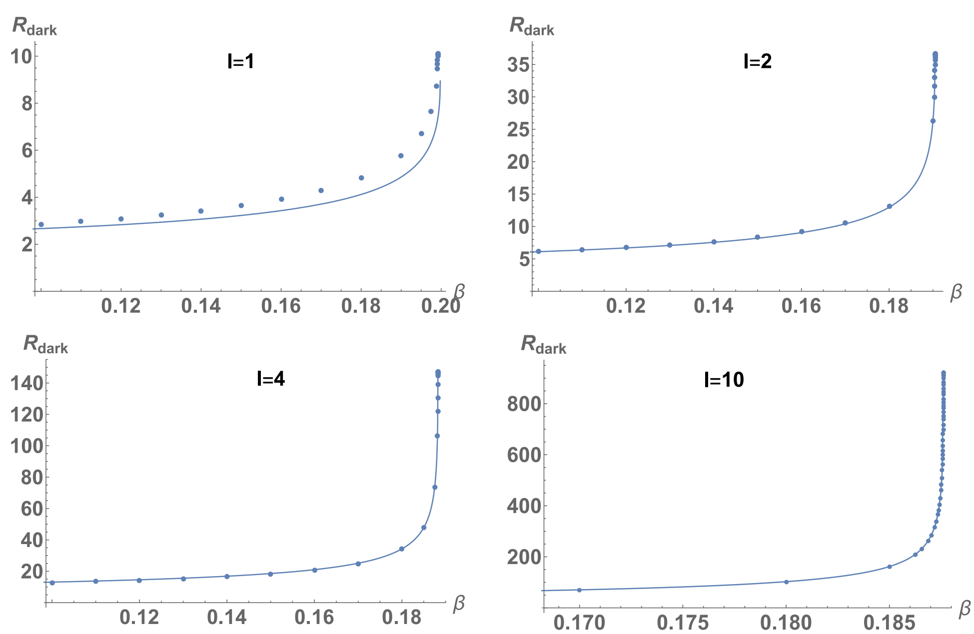

Fig. 5. The radius of the infinite vortex solution as a function of the propagation constant β for different values of l. We show a comparison of the formula obtained from the variational model (36) (solid lines) to some values found by direct numerical computation of the vortices.

of Section 3. In particular, using (23) and (36), we can see that the radii of the dark regions coincide:

$$\lim_{R_{ext}\to\infty} R_{int} = \lim_{\beta\to\beta_{cr}} R_{dark} = \frac{8l^2}{\sqrt{3}} \tag{39}$$

4.2. Stability

The azimuthal stability of the dark soliton families can be analysed in a similar way as was done for the vortex solitons [18]. The stationary states of charge l, $\Psi(r,z)$, are perturbed by small functions with a p-order azimuthal symmetry,

$$\tilde{\Psi}(r,\theta,z) = [\Psi(r,z) + F(r,z)\exp(ip\theta) + \\ + G(r,z)\exp(-ip\theta)]\exp[i(l\theta+\beta z)], \tag{40}$$

where

$$F(r,z) = f(r)\exp(\delta z) \tag{41}$$

$$G(r,z) = g(r)\exp(\delta^* z). \tag{42}$$

Replacing this perturbed state into Eq. (1) and keeping only terms of first order (linearization) a set of coupled equations for

$F(r,z)$ and $G(r,z)$ is obtained and can be written in the form,

$$i\frac{\partial}{\partial z}\begin{pmatrix} F \\ -G^* \end{pmatrix} = -\mathcal{A}\begin{pmatrix} F \\ G^* \end{pmatrix}, \tag{43}$$

being $\mathcal{A}$ the operator,

$$\mathcal{A} = \begin{pmatrix} \nabla_r^2 - \frac{(l+p)^2}{r^2} + Q & R \\ R & \nabla_r^2 - \frac{(l-p)^2}{r^2} + Q \end{pmatrix}, \tag{44}$$

and where $\nabla_r^2 \equiv \partial_r^2 + (1/r)\partial_r$, $Q = -\beta + (2 - 3\psi^2)\psi^2$ and $R = (1 - 2\psi^2)\psi^2$. The perturbation eigenstates can be obtained applying a finite difference scheme to the problem (43) and carry out propagation steps repeatedly up to the point the growth rate of the field vector $(f|g^*)^T$ reaches a fixed value. From the growth rate at any step a guess for δ can be obtained. This was the method used in [18,45] and basically constitutes a variant of the direct power method. Convergence is slow and requires from a quite long propagation distance, particularly when the growth rate is close to zero. At such condition it is also necessary to use short steps Δz in order to avoid precision errors. According to this we decided to use a more straightforward and reliable method to solve for the required eigenvalues.

Replacing Eqs (41) and (42) in Eq. (43) we get the following generalized eigenvalue problem,

$$\mathcal{A}\begin{pmatrix} f \\ g^* \end{pmatrix} = (i\delta)\mathcal{B}\begin{pmatrix} f \\ g^* \end{pmatrix} \tag{45}$$

where $(i\delta)$ is the eigenvalue, $\mathcal{A}$ is the same matrix defined in (44) and $\mathcal{B}$ comes given by,

$$\mathcal{B} = \begin{pmatrix} -I & 0 \\ 0 & I \end{pmatrix} \tag{46}$$

being I the identity operator. A finite difference scheme is then applied to the problem discretizing the variable r, as well as functions $f(r)$ and $g^*(r)$ into n samples to get a matrix algebraic problem of order $2n$. Matrix $\mathcal{A}$ is real but non-symmetric which means there can exist eigensolutions in the form of complex conjugate pairs. Those are actually the interesting ones since the imaginary part correspond to the real part of δ which accounts for the growth rate of the perturbation. In fact, the existence of conjugate pairs is in accordance to the propagation direction inversion symmetry which means that the stable or unstable character of a particular state should not depend on whether it propagates along z or $-z$ direction.

The problem (45) was solved for different values of the charge l ($l = 1, 2, 3, 4$ and 10) and different perturbation orders p ranging from 1 to 8 (cases $l = 1, 2, 3$ and 4) and from 1 to 15 (case $l = 10$). In all cases a broad domain of β, from $\beta = 0.01$ to $\beta = \beta_{cr}$ was scanned, carrying out the calculation in about 80 or 90 distributed points. In none of the cases a complex eigenvalue was obtained, revealing all those values of $(i\delta)$ are real and consequently all values of δ are purely imaginary. This means that all checked state families remain azimuthally stable for all the perturbations analysed. It is expected that the stable character will remain for other larger perturbations as the term $-(l \pm p)^2/r^2$ in the operator makes the effective potential increasingly negative for increasing values of p.

Also, simulations to propagate a number of eigenstates after including numerical noise were also carried out and they remained stable in all the cases. All this makes us to conclude with a great deal of confidence that dark soliton solutions are stable for any value of β and probably for any angular momentum. This conclusion substantially generalizes the result of [43], where the stability of the dark solitons was only discussed for a limited range of solutions.

5. Conclusions

The main results of this work can be summarized as follows:

- We have developed a variational procedure that allowed us to write down an effective Hamiltonian or Lagrangian for a spinning wavefunction in its liquid-like phase in terms of physically recognizable terms: a bulk density, a surface tension and a centrifugal term. We have shown that it yields a good approximation to the profiles and shapes of vortex and dark solitons. The method was implemented for the two-dimensional cubic–quintic model but it might prove useful in other situations with flat-top solutions, such as the three dimensional version of the model [17,46] or for other physical settings like quantum droplets [29,30].
- We have presented the dark soliton solutions of the cubic–quintic model and found an l-dependent eigenvalue cutoff.
- We have studied the azimuthal stability of the solutions by a linear analysis finding that all of them are stable al least for $l = 1, 2, 3, 4$ and 10. It is expected that this stable character remains for other values of the angular momentum.
- We have derived the explicit form of the Pohozaev identity for an infinite NLSE fluid with angular momentum and used it to discard the existence of solutions with an asymptotic behaviour which is seemingly allowed if we just look at the large r region.

Declaration of competing interest

The authors declare that they have no known competing financial interests or personal relationships that could have appeared to influence the work reported in this paper.

Acknowledgements

This publication is part of the R&D&i project PID2020-118613GB-I00, funded by MCIN/AEI/10.13039/501100011033/. This work was also supported by grant ED431B 2021/22 (Xunta de Galicia).

Appendix. Pohozaev identity and non-existence of dark solitons asymptoting to $\psi_{\infty,-}$.

In this appendix we will derive the explicit form of the Pohozaev identity [47,48] for the dark soliton solutions of Section 4, namely for Eq. (7) with boundary condition $\lim_{r\to\infty}\psi = \psi_{\infty,\pm}$ where $\psi_{\infty,\pm}$ are given in Eq. (14). Then, we use this identity to demonstrate that solutions such that $\lim_{r\to\infty}\psi(r) = \psi_{\infty,-} = \frac{1-\sqrt{1-4\beta}}{2}$ do not exist.[5] Finally, we briefly comment on how the identity is satisfied by the variational profiles introduced in Section 4.1 that asymptote to $\psi_{\infty,+}$.

We start by rewriting Eq. (7) as:

$$(r\psi')' - \frac{l^2}{r}\psi + rf(\psi) = 0 \tag{47}$$

where we have defined:

$$f(\psi) = -\beta\psi + \psi^3 - \psi^5 \tag{48}$$

We can express Eq. (47) multiplied by $r\psi'$ as:

$$\frac{1}{2}(r^2\psi'^2)' - l^2\psi\psi' + r^2 f(\psi)\psi' = 0 \tag{49}$$

[5] It is worth mentioning that in [40], Pohozaev's identity was used to prove that there is an eigenvalue cutoff $\beta < \beta_{cr}$ in the case of solutions of Eq. (5) that decay to zero at infinity.

Now, consider functions $F_\pm(\psi)$ for both types of boundary conditions such that $\frac{dF_\pm}{d\psi} = f$ and $F_\pm(\psi_{\infty,\pm}) = 0$, namely:

$$F_\pm(\psi) = -\frac{1}{2}\beta\psi^2 + \frac{1}{4}\psi^4 - \frac{1}{6}\psi^6 + \frac{1}{2}\beta\psi_{\infty,\pm}^2 - \frac{1}{4}\psi_{\infty,\pm}^4 + \frac{1}{6}\psi_{\infty,\pm}^6 = \\ = -\frac{1}{6}(\psi^2 - \psi_{\infty\pm}^2)^2\left(\psi^2 - \left(\frac{1}{2} \mp \sqrt{1-4\beta}\right)\right) \quad (50)$$

Notice that, by construction, we have required that $F(\psi_\infty) = 0$ and $\frac{dF}{d\psi}|_{\psi=\psi_\infty} = f(\psi_\infty) = 0$. Therefore, F has a double zero at ψ_∞ in general. This can be explicitly seen in (50) for the cubic–quintic case but the same would hold for any nonlinear potential as long as F can be Taylor-expanded around ψ_∞.

Using that $\frac{dF_\pm}{dr} = f\psi'$, Eq. (49) can be rewritten as:

$$(r^2\psi'^2)' - l^2(\psi^2)' + (2r^2F_\pm)' - 4rF_\pm = 0 \quad (51)$$

Let us now integrate this expression from $r = 0$ to $r = \infty$. The first three terms are total derivatives and therefore give rise to boundary terms. In order to determine them, the next step is to understand the asymptotic behaviour of $\psi(r)$ at $r = 0$ and $r = \infty$. Being a vortex of order l, $\psi(r)$ is proportional to r^l near $r = 0$ and it is immediate to check that the three boundary contributions vanish in this region. On the other hand, the $r \to \infty$ limit of ψ can be obtained by expanding the equation and we find that, assuming $l \neq 0$, the difference $\psi - \psi_\infty$ decays as r^{-2}:

$$\psi = \psi_\infty\left(1 + l^2\left(\frac{df}{d\psi}\bigg|_{\psi=\psi_\infty}\right)^{-1} r^{-2} + \mathcal{O}(r^{-4})\right) \quad (52)$$

Taking into account this expression and the double zero for $F_\pm$ at $\psi_{\infty,\pm}$, see Eq. (50), the $F_\pm$ decays as r^{-4} for large r. Therefore, the only non-vanishing boundary contribution for the integral of (51) comes from the second term. The sought Pohozaev identity is:

$$\int_0^\infty rF_\pm dr = -\frac{1}{4}l^2\psi_{\infty,\pm}^2 \quad (53)$$

We will see now that this Pohozaev identity allows us to easily prove that there cannot be regular solutions of (7) such that $\lim_{r\to\infty}\psi(r) = \psi_{\infty,-}$. The point is that, in this case, the function F in (50) takes the form:

$$F_- = -\frac{1}{6}(\psi^2 - \psi_{\infty,-}^2)^2(\psi^2 - \psi_F^2) \quad (54)$$

where $\psi_F^2 = \frac{1}{2} + \sqrt{1-4\beta}$. Notice that $\psi_F^2 > \psi_{\infty,+}^2 > \psi_{\infty,-}^2$. For any value $\psi^2 < \psi_F^2$, the function F_- is positive. On the other hand, the Pohozaev identity tells us that the integral of rF_- is a negative number. If this is to be fulfilled, ψ should grow larger than ψ_F at some value of r. Then, it should reach a maximum and go back down to $\psi_{\infty,-}$. But from the Eq. (7) itself, we see that this is impossible. At the maximum, we would have $\psi' = 0$ and $\psi'' < 0$. This would mean $\frac{l^2}{r^2}\psi + \beta\psi - \psi^3 + \psi^5 < 0$. However, $\beta\psi - \psi^3 + \psi^5 < 0$ is negative only in the interval $\psi_{\infty,-} < \psi < \psi_{\infty,+}$ and therefore cannot be negative for any $\psi > \psi_F$. It is impossible that ψ becomes larger that ψ_F and then starts decreasing at a larger value of r. Thus, no solutions asymptoting to $\psi_{\infty,-}$ exist.

We close this appendix by analysing the physical solutions asymptoting to $\psi_{\infty,+}$ from the point of view of the variational profile discussed in Section 4.1. We can split the integral in (53) in three regions: In the vortex hole, $r \le R_{dark}$, we have $\psi \approx 0$ and therefore $F_+ \approx C$ where we introduce:

$$C = \frac{1}{2}\beta\psi_{\infty,+}^2 - \frac{1}{4}\psi_{\infty,+}^4 + \frac{1}{6}\psi_{\infty,+}^6 \quad (55)$$

The contribution to the integral $\int rF_+dr$ is $\frac{1}{2}R_{dark}^2C$. For $r \ge R_{dark}$, we have $\psi \approx \psi_\infty$ and therefore $F \approx 0$ and there is no contribution to the integral. Then we have the kink region $\int rF_+dr \approx R_{dark}\int F_{kink} \approx -\frac{1}{8}R_{dark}\psi_\infty^3\sqrt{1-\psi_\infty^2}$ where we have used the variational profile (27) with the value of a derived in Eq. (33). Summing the three contributions, we can write the Pohozaev identity as:

$$\frac{1}{2}R_{dark}^2C - \frac{1}{8}R_{dark}\psi_{\infty,+}^3\sqrt{1-\psi_{\infty,+}^2} = -\frac{l^2\psi_{\infty,+}^2}{4} \quad (56)$$

Using the value of C given in (55) and the value of $\psi_{\infty,+}$ written in (14), we can check that the solutions of this quadratic equation are precisely (36).

References

[1] L.M. Pismen, Vortices in Nonlinear Fields: From Liquid Crystals to Superfluids, from Non-Equilibrium Patterns to Cosmic Strings, Vol. 100, Oxford University Press, 1999.

[2] J. Nye, M. Berry, Dislocations in wave trains, in: Proceedings of the Royal Society of London a: Mathematical, Physical and Engineering Sciences, Vol. 336, The Royal Society, 1974, pp. 165–190.

[3] P. Coullet, L. Gil, F. Rocca, Optical vortices, Opt. Commun. 73 (5) (1989) 403–408.

[4] M. Uchida, A. Tonomura, Generation of electron beams carrying orbital angular momentum, Nature 464 (7289) (2010) 737–739.

[5] J. Abo-Shaeer, C. Raman, J. Vogels, W. Ketterle, Observation of vortex lattices in bose-einstein condensates, Science 292 (5516) (2001) 476–479.

[6] A.S. Desyatnikov, Y.S. Kivshar, L. Torner, Optical vortices and vortex solitons, in: Progress in Optics, vol. 47, Elsevier, 2005, pp. 291–391, http://dx.doi.org/10.1016/S0079-6638(05)47006-7, (Chapter 5). URL https://www.sciencedirect.com/science/article/pii/S0079663805470067.

[7] N. Parker, B. Jackson, A. Martin, C. Adams, Vortices in bose-einstein condensates: theory, in: Emergent Nonlinear Phenomena in Bose–Einstein Condensates, Springer, 2008, pp. 173–189.

[8] C. Sulem, P.-L. Sulem, The Nonlinear Schrödinger Equation: Self-Focusing and Wave Collapse, Vol. 139, Springer Science & Business Media, 2007.

[9] Y.V. Kartashov, G.E. Astrakharchik, B.A. Malomed, L. Torner, Frontiers in multidimensional self-trapping of nonlinear fields and matter, Nat. Rev. Phys. 1 (3) (2019) 185–197.

[10] Á. Paredes, D. Feijoo, H. Michinel, Coherent cavitation in the liquid of light, Phys. Rev. Lett. 112 (17) (2014) 173901.

[11] B.A. Malomed, Vortex solitons: Old results and new perspectives, Physica D 399 (2019) 108–137.

[12] B. Malomed, L.-C. Crasovan, D. Mihalache, Stability of vortex solitons in the cubic-quintic model, Physica D 161 (3–4) (2002) 187–201.

[13] A. Paredes, J. Blanco-Labrador, D.N. Olivieri, J.R. Salgueiro, H. Michinel, Vortex revivals and fermi-pasta-ulam-tsingou recurrence, Phys. Rev. E 99 (6) (2019) 062211.

[14] Y.S. Kivshar, B. Luther-Davies, Dark optical solitons: physics and applications, Phys. Rep. 298 (2–3) (1998) 81–197.

[15] M. Quiroga-Teixeiro, H. Michinel, Stable azimuthal stationary state in quintic nonlinear optical media, J. Opt. Soc. Amer. B 14 (8) (1997) 2004–2009.

[16] I. Towers, A.V. Buryak, R.A. Sammut, B.A. Malomed, L.-C. Crasovan, D. Mihalache, Stability of spinning ring solitons of the cubic–quintic nonlinear schrödinger equation, Phys. Lett. A 288 (5–6) (2001) 292–298.

[17] D. Mihalache, D. Mazilu, L.-C. Crasovan, I. Towers, A. Buryak, B. Malomed, L. Torner, J. Torres, F. Lederer, Stable spinning optical solitons in three dimensions, Phys. Rev. Lett. 88 (7) (2002) 073902.

[18] H. Michinel, J.R. Salgueiro, M.J. Paz-Alonso, Square vortex solitons with a large angular momentum, Phys. Rev. E 70 (6) (2004) 066605.

[19] H. Michinel, J. Campo-Táboas, R. García-Fernández, J. Salgueiro, M. Quiroga-Teixeiro, Liquid light condensates, Phys. Rev. E 65 (6) (2002) 066604.

[20] S. Xiang, L. Hua-Mei, Exact solutions of the two-dimensional cubic-quintic nonlinear schrödinger equation with spatially modulated nonlinearities, Commun. Theor. Phys. 59 (3) (2013) 290.

[21] C. Zhou, X. He, Stochastic diffusion of electrons in evolutive langmuir fields, Phys. Scr. 50 (4) (1994) 415.

[22] C. Josserand, S. Rica, Coalescence and droplets in the subcritical nonlinear schrödinger equation, Phys. Rev. Lett. 78 (7) (1997) 1215.

[23] F. Smektala, C. Quemard, V. Couderc, A. Barthélémy, Non-linear optical properties of chalcogenide glasses measured by z-scan, J. Non-Crystalline Solids 274 (1–3) (2000) 232–237.

[24] H. Michinel, M.J. Paz-Alonso, V.M. Pérez-García, Turning light into a liquid via atomic coherence, Phys. Rev. Lett. 96 (2) (2006) 023903.

[25] S.-C. Tian, R.-G. Wan, C.-Z. Tong, Y.-Q. Ning, Giant fifth-order nonlinearity via tunneling induced quantum interference in triple quantum dots, AIP Adv. 5 (2) (2015) 027111.

[26] Z. Wu, Y. Zhang, C. Yuan, F. Wen, H. Zheng, Y. Zhang, M. Xiao, Cubic-quintic condensate solitons in four-wave mixing, Phys. Rev. A 88 (6) (2013) 063828.
[27] L.R. Kassab, C.D. Bordon, A.S. Reyna, C.B. de Araújo, Nanoparticles-based photonic metal–dielectric composites: A survey of recent results, Opt. Mater. X 12 (2021) 100098.
[28] D. Petrov, Quantum mechanical stabilization of a collapsing bose-bose mixture, Phys. Rev. Lett. 115 (15) (2015) 155302.
[29] C. Cabrera, L. Tanzi, J. Sanz, B. Naylor, P. Thomas, P. Cheiney, L. Tarruell, Quantum liquid droplets in a mixture of bose-einstein condensates, Science 359 (6373) (2018) 301–304.
[30] Z.-H. Luo, W. Pang, B. Liu, Y.-Y. Li, B.A. Malomed, A new form of liquid matter: Quantum droplets, Front. Phys. 16 (3) (2021) 1–21.
[31] K.I. Pushkarov, D. Pushkarov, I. Tomov, Self-action of light beams in nonlinear media: soliton solutions, Opt. Quantum Electron. 11 (6) (1979) 471–478.
[32] W.-S. Kim, H.-T. Moon, Soliton-kink interactions in a generalized nonlinear schrödinger system, Phys. Lett. A 266 (4–6) (2000) 364–369.
[33] Z. Birnbaum, B.A. Malomed, Families of spatial solitons in a two-channel waveguide with the cubic-quintic nonlinearity, Physica D 237 (24) (2008) 3252–3262.
[34] R.L. Pego, H.A. Warchall, Spectrally stable encapsulated vortices for nonlinear schrödinger equations, J. Nonlinear Sci. 12 (4) (2002) 347–394.
[35] T. Davydova, A. Yakimenko, Stable multicharged localized optical vortices in cubic–quintic nonlinear media, J. Opt. A: Pure Appl. Opt. 6 (5) (2004) S197.
[36] A.L. Fetter, Rotating trapped bose-einstein condensates, Rev. Modern Phys. 81 (2) (2009) 647.
[37] R.Y. Chiao, E. Garmire, C.H. Townes, Self-trapping of optical beams, Phys. Rev. Lett. 13 (15) (1964) 479.
[38] M. Desaix, D. Anderson, M. Lisak, Variational approach to collapse of optical pulses, J. Opt. Soc. Amer. B 8 (10) (1991) 2082–2086.
[39] J. Qin, G. Dong, B.A. Malomed, Stable giant vortex annuli in microwave-coupled atomic condensates, Phys. Rev. A 94 (5) (2016) 053611.
[40] V. Prytula, V. Vekslerchik, V.M. Perez-Garcia, Eigenvalue cutoff in the cubic-quintic nonlinear schrödinger equation, Phys. Rev. E 78 (2) (2008) 027601.
[41] R.M. Caplan, R. Carretero-González, P.G. Kevrekidis, B.A. Malomed, Existence, stability, and scattering of bright vortices in the cubic–quintic nonlinear schrödinger equation, Math. Comput. Simulation 82 (7) (2012) 1150–1171.
[42] D. Novoa, H. Michinel, D. Tommasini, Pressure, surface tension, and dripping of self-trapped laser beams, Phys. Rev. Lett. 103 (2) (2009) 023903.
[43] V. Berezhiani, V. Skarka, N. Aleksić, Dynamics of localized and nonlocalized optical vortex solitons in cubic-quintic nonlinear media, Phys. Rev. E 64 (5) (2001) 057601.
[44] K. Dimitrevski, E. Reimhult, E. Svensson, A. Öhgren, D. Anderson, A. Berntson, M. Lisak, M.L. Quiroga-Teixeiro, Analysis of stable self-trapping of laser beams in cubic-quintic nonlinear media, Phys. Lett. A 248 (5–6) (1998) 369–376.
[45] J.M. Soto-Crespo, D.R. Heatley, E.M. Wright, N.N. Akhmediev, Stability of the higher-bound states in a saturable self-focusing medium, Phys. Rev. A 44 (1991) 636–644, http://dx.doi.org/10.1103/PhysRevA.44.636, URL https://link.aps.org/doi/10.1103/PhysRevA.44.636.
[46] D. Mihalache, D. Mazilu, L.-C. Crasovan, B. Malomed, F. Lederer, Three-dimensional spinning solitons in the cubic-quintic nonlinear medium, Phys. Rev. E 61 (6) (2000) 7142.
[47] S. Pohozaev, Eigenfunctions of the equation $\delta u + f(u) = 0$, in: Dokl. Akad. Nauk SSSR, Vol. 165, 1965, pp. 33–36.
[48] H. Berestycki, P.-L. Lions, Nonlinear scalar field equations, i existence of a ground state, Arch. Ration. Mech. Anal. 82 (4) (1983) 313–345.